Symmetric and adjustable phase of higher-order reflected light from two-dimensional photonic crystal

Qiao-Feng Dai,[1,*] Sheng Lan,[1] and He-Zhou Wang[2]

[1]*Laboratory of Photonic Information Technology, School for Information and Optoelectronic Science and Engineering, South China Normal University, Guangzhou 510006, China*
[2]*State Key Laboratory of Optoelectronic Materials and Technologies, Zhongshan (Sun Yat-Sen) University, Guangzhou 510275, China*
[*]*Corresponding author: daiqf@scnu.edu.cn*

Received September 3, 2009; revised November 19, 2009; accepted December 17, 2009; posted December 22, 2009 (Doc. ID 116071); published February 2, 2010

Investigation on the phase shifts of higher-order reflected light from a two-dimensional photonic crystal (PC) demonstrates that the phase shift of $-m$th order reflected light is symmetric with respect to the line of $k_x = m\pi/b$ in the frequency-wave vector domain, where k_x and b denote the incident wave vector component along the surface and the period of the PC along the surface, respectively, and m is an integer. Such phase symmetry originates from the periodicity of a PC along the surface. When higher-order propagating waves appear between two band edges of a stop band, the phase change of the 0th order reflection is generally not π as reported before. Moreover, the reflection phase can be adjusted and designed by changing the cylinder radii of the surface layer. It provides a robust way to achieve a giant Goos–Hänchen shift, which is described in detail as an example, and superluminal propagation from a PC. © 2010 Optical Society of America

OCIS codes: 050.5298, 050.5080, 120.5700.

1. INTRODUCTION

Photonic crystals (PCs) are artificial structures consisting of periodic arrays of dielectric or metal materials. The unique properties of PCs have been extensively researched. Amplitude, frequency, and phase are three important parameters indicating the characteristics of light. So far, most investigations of PCs have been made on the amplitude and frequency of transmitted or reflected light. By comparison, investigations on the phase properties are relatively few.

Many important physical phenomena are correlated with phase shift ϕ of transmitted or reflected waves. Among them, superluminal (faster-than-light) phenomena, attracting much attention of physicists for their mysterious physical hypostasis [1–3], can be characterized by $d\phi(\omega)/d\omega$ [4–7]. Another interesting phenomenon is the Goos–Hänchen (GH) effect, which refers to the lateral shift of a totally reflected wave beam from the path usually expected from geometrical optics. The GH shift can be calculated analytically as $-d\phi(k_x)/dk_x$ [8–14], where k_x is the incident wave vector component along the interface. The well-designed phase is the key to achieve superluminal propagation and a giant GH shift from a PC.

Recently, the phase properties of the 0th order reflection wave from PCs have been investigated when all the higher-order reflection waves are evanescent waves. Some researchers reported that in the case of normal incidence, the 0th order reflection phase shift is π between two band edges of the stop band [15–18]. Using the phase property of TE and TM waves reflected from a 2D PC, a kind of broadband phase retarder is proposed [19]. On the other hand, the diffraction efficiency of PCs, which is the energy flux of higher-order reflection light, is researched [20–22]. However, the phase characteristics of higher-order reflection light from PCs have not yet been revealed.

In this paper, the phase properties of higher-order reflection light from a 2D PC are revealed systematically, and the phase shifts can be adjusted and designed. From these phase properties many applications can be developed. As an example, the giant GH shift is described.

2. THEORY

Before calculation, we would like to discuss the wave vector matching condition at the interface of a PC structure. This condition is represented in the conservation of the parallel component to the interface of the wave vector. It can been generalized to $k_{\parallel}=k_x+G_m=k_x+2\pi m/b$, where m is an integer equal to 0, ±1, ±2, etc.; b represents the period of the PC along the surface, and b is not always equal to the lattice constant [20,21]; and k_x and $k_{\parallel}$ are parallel to the interface component of the incident and the reflective wave vector, respectively. The mth order reflective wave is able to propagate only when $\omega > |k_x + 2\pi m/b|c/n_{\mathrm{in}}$, or else it is evanescent, where n_{in} is the refractive index of incident medium. With bigger values of b and n_{in}, the more higher-order waves are propagable in a lower frequency domain.

For demonstration, the transfer matrix method [23] (TMM) is employed to obtain the phase shifts of TE or TM waves reflected from a 2D PC. The complex reflection co-

efficient can be defined as $r=u_r/u_{\text{in}}$, where u_r is the field of the reflected wave and u_{in} is the field of the incident wave. The mth order complex reflection coefficient can be extracted as

$$r^{(m)} = \frac{u_r^{(m)}}{u_{\text{in}}} = |r^{(m)}|e^{i\phi^{(m)}}, \tag{1}$$

where $\phi^{(m)}$ is the mth order phase shift of the reflected wave from a 2D PC. We investigate a 2D air cylinder PC whose unit cell is air cylinders embedded in a substrate medium. The structure (shown in Fig. 1) is a square lattice with a lattice constant of a. r denotes the radius of the air cylinder. The thickness of the PC along the z direction is L. n_0 and n_{in} are the refractive index of air and the substrate medium, respectively. Here, $b=a$ along the Γ-X direction of the square lattice. We set $r=0.5a$, $L=10a$, $n_0=1.0$, and $n_{\text{in}}=3.4$. An Si substrate ($n_{\text{in}}=3.4$) with a high refractive index is adopted to make more higher-order waves propagable in a lower frequency domain. For a TM wave (i.e., the electric field vector is parallel to the cylinders), Fig. 2 shows the intensities and phases of different-order reflected waves in the (ω,k_x) plane, where ω is the frequency of the plane wave and k_x is the wave vector component of the incident light along the interface (i.e., x direction). Among them, Figs. 2(a1)–2(c1) are the intensities of the 0th, −1st, and −2nd order reflected waves, respectively; Figs. 2(a2)–2(c2) are the corresponding phases. Since we are more interested in the phase of a propagating reflected wave, the field values of the region, where either the incident or the reflected waves are evanescent waves, are set to zero for the reflectance and reflection phase in the (ω,k_x) plane. Those are displayed in the down-right or down-left corner in Figs. 2(a1)–2(c1) and Figs. 2(a2)–2(c2). The incident wave is an evanescent wave inside the down-right dark corner, and the reflected wave is an evanescent wave inside the two dark corners, if they exist. The propagating region is over the two regions. In the (ω,k_x) plane, line $k_x(a/\pi)=0$ is corresponding to normal incident light, while line $\omega(a/2\pi c)=k_x(a/\pi)/6.8$ [the dashed lines in Figs. 2(a1)–2(c1)] is the light line corresponding to the incident angle of 90 degrees. Here, $\omega a/2\pi c$ is defined as a normalized frequency. In order to show the relationship more directly, the dependence of the phase on k_x in a fixed frequency are presented in Figs. 2(a3)–2(c3). Among them, Fig. 2(a3) presents the 0th reflection phase in a normalized frequency of 0.315, Fig. 2(b3) presents the −1st reflection phase in a normalized frequency of 0.315, and Fig. 2(c3) presents the −2nd reflection phase in a normalized frequency of 0.552. The corresponding frequencies are marked in Figs. 2(a2)–2(c2) with dashed lines.

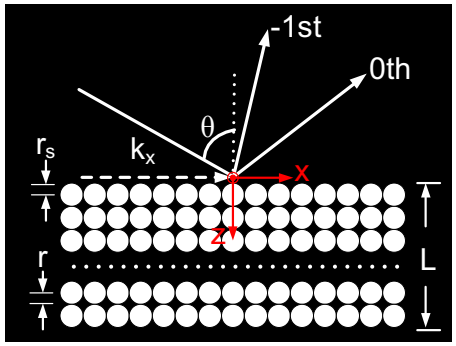

Fig. 1. (Color online) Schematic diagram of incident and reflected light on a PC structure of square lattice. The black and white denote the substrate medium and air cylinders, respectively.

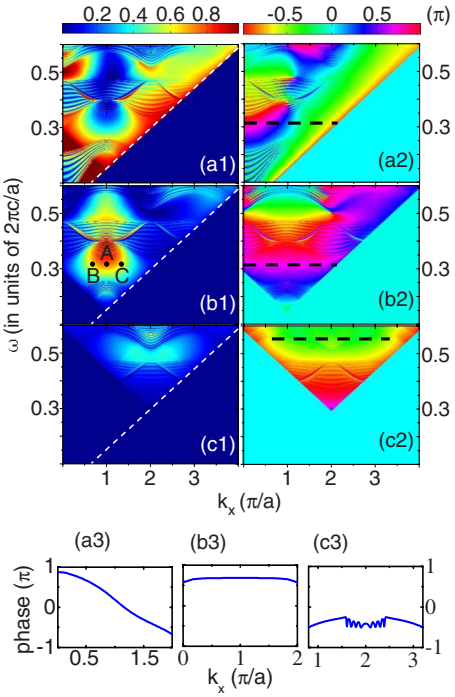

Fig. 2. (Color online) (a1)–(c1) are reflectance of the 0th, −1st and −2nd order reflected waves as functions of frequency and k_x, respectively. (a2)–(c2) are reflection phase of the 0th, −1st, and −2nd order reflected waves as functions of frequency and k_x, respectively. (a3) Presents the 0th reflection phase in normalized frequency of 0.315, (b3) presents the −1st reflection phase in normalized frequency of 0.315, and (c3) presents the −2nd reflection phase in normalized frequency of 0.552. The corresponding frequencies are marked in (a2)–(c2) with dashed lines. The PC structure (Fig. 1) with $r=r_s=0.5a$. Points A, B, and C have the same frequency in (b1).

As we know, for a metallic grating the diffraction properties for two polarizations are different from each other regarding the excited surface plasma of metal. However, for a 2D PC consisting of dielectric materials, the reflective properties of a TE wave are similar to those of a TM wave. Therefore, in the following we only represent those of a TM wave.

3. THE PROPERTIES OF REFLECTION PHASE

The most obvious property in Fig. 2 is symmetry; the phase shift of the $-m$th order reflective light is symmetric with respect to line $k_x=m\pi/b$ in the frequency-wave vector domain. For the −1st order reflected wave, the intensity and phase are symmetric with respect to line $k_x=\pi/a$ in the frequency-wave vector domain for $0<k_x<2\pi/a$. For the −2nd order reflected wave, the intensity and phase are symmetric with respect to line $k_x=2\pi/a$ in the frequency-wave vector domain for $0<k_x<4\pi/a$. It can be achieved that the phase shift of the $-m$th order re-

flected light is symmetric with respect to line $k_x = m\pi/a$ in the frequency-wave vector domain for $0 < k_x < 2m\pi/a$. The intensity and phase of the 0th order wave are unsymmetrical in the frequency-wave vector domain, and so are the +1st and +2nd order wave (not presented in this paper). To show the physical meaning of symmetry clearly, the −1st order reflected wave is investigated as a sample. Three points in Fig. 2(b1) are labelled with A, B, and C whose corresponding k_x are π/a, $\pi/a-\Delta k$, and $\pi/a+\Delta k$, respectively. Points B and C are symmetric with respect to line $k_x = \pi/a$, and point A is in the symmetric line $k_x = \pi/a$. The sketches of reflection in three points are shown in Fig. 3. In point A, when a light with wave vector $k_x = \pi/a$ is incident to a PC, the −1st order reflected wave with $k_x = \pi/a - 2\pi/a = -\pi/a$ propagates back along the incident direction, as shown in Fig. 3(a). In point B, as a light with $k_x = \pi/a - \Delta k$ is incident into a PC, shown in Fig. 3(b), the −1st order reflection coefficient is set to be r_B. In point C, as a light with $k_x = \pi/a + \Delta k$ is incident into a PC, shown in Fig. 3(c), the −1st order reflection coefficient is set to be r_C. There are two interesting characteristics appearing. First, it is not difficult to find that the incident direction in point C is inverse to the −1st order reflective direction in point B, while the −1st order reflective direction in point C is inverse to the incident direction in point B. Second, r_B is equal to r_C from the symmetry of Figs. 2(b1) and 2(b2). These characteristics cannot be simply deduced by the principle of reversibility, since many higher-order propagating waves are present in reflection. We also calculate the phase shift of a PC with only one layer of cylinder, more like a grating, and the symmetry also remains. The symmetries of the reflection phase and reflectance originate from the displacement periodicity along the surface of the PC.

From one band edge to the other inside the stop band, the change of the reflection phase is not π identically. With only the 0th order propagating wave, the reflection phase changes from 0 to π when going from one band edge to the other one in the case of normal incidence [15–18]. In general, when a higher-order wave is propagating, as in our case, the reflection phase becomes complicated inside the bandgap. For simplicity, we consider the 0th order wave of Figs. 2(a1) and 2(a2). With normal incidence ($k_x = 0$), the total reflected energy flux as a function of a normalized frequency is shown in Fig. 4(a), and the reflectance and the reflection phase of the 0th order reflected wave as functions of a normalized frequency are plotted in Figs. 4(b) and 4(c), respectively. The change of the reflection phase plotted in Fig. 4(c) is 1.1π across the first bandgap, while it is 0.4π across the second bandgap. As the incident angle is close to 90 degree, the reflectance is high even in the pass band for the 0th reflected wave in Fig. 2(a1), and the reflection phase is about -0.85π in the whole frequency domain shown in Fig. 2(a2). Similar phenomena appear in total internal reflection when an incident angle is bigger than a critical angle. That is not surprising since the refractive index of an incident medium is larger than the average refractive index of a PC. We have also calculated the phase for different structure and lattice constants. It is found that the phase change between two band edges of a stop band of the 0th order reflection is not π, in general, as higher-order propagating waves are appearing.

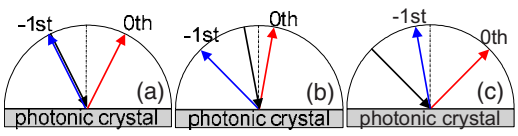

Fig. 3. (Color online) (a)–(c) Sketches of reflection in points A, B, and C of Fig. 2(b1), respectively. Lines with arrows indicate the wave vectors of incident, the 0th, and the −1st order reflected lights, respectively.

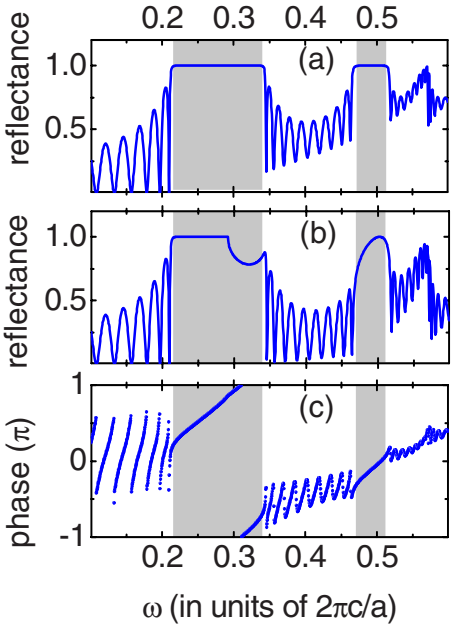

Fig. 4. (Color online) With normal incidence, i.e., $k_x = 0$, (a) is the reflected energy flux including all order propagating waves as a function of frequency; (b) and (c) are reflectance and phase of the 0th reflected wave as functions of frequency, respectively. The reflection bands, in which the total reflection energy flux is greater than 99.9%, are shown by shaded areas.

The phase can be modulated by modifying the surface layer. We investigate a 2D PC with almost the same structure as that in Fig. 2. The only difference is that the radii of the surface layer cylinders are set to $0.4a$. The reflectance and the reflection phase are shown in Fig. 5. Among them, Figs. 5(a1)–5(c1) are the intensity of the 0th, −1st, and −2nd order reflected waves, respectively; Figs. 5(a2)–5(c2) are the corresponding phases. Figure 5(a3) presents the 0th reflection phase in the normalized frequency of 0.315, Fig. 5(b3) presents the −1st reflection phase in the normalized frequency of 0.315, and Fig. 5(c3) presents the −2nd reflection phase in the normalized frequency of 0.552. The phase is fully changed inside the stop band, and the reflected energy flux redistributes among the different reflected orders. A most obvious change is the concave that appears inside the first stop band of the 0th order and −1st order. The phase and reflectance near to the concave vary drastically in the (ω, k_x) plane. As mentioned above, it is possible to achieve superluminal propagation and a giant GH shift near the concave. As the strongest field localizes in a PC surface inside the stop band generally, the phase is sensitive to perturbation of surface layer. When the radii of the cylinders in the surface layer are changed, the phase will change accordingly. It is

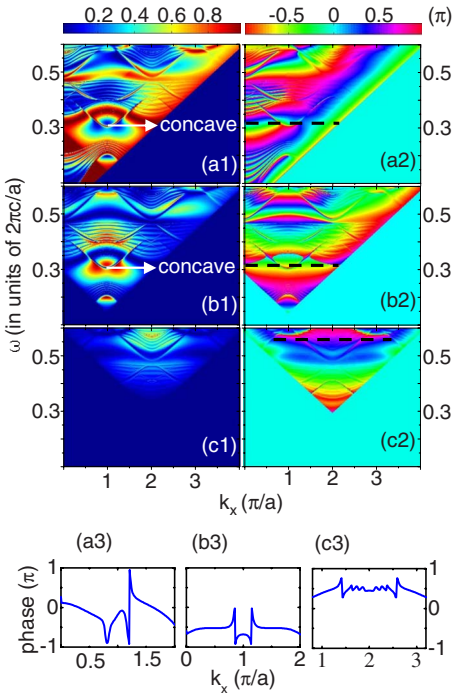

Fig. 5. (Color online) (a1)–(c1) Reflectance of the 0th, −1st, and −2nd order reflected waves as functions of frequency and k_x, respectively. (a2)–(c2) Reflection phase of the 0th, −1st, and −2nd order reflected waves as functions of frequency and k_x, respectively. (a3) Presents the 0th reflection phase in normalized frequency of 0.315, (b3) presents the −1st reflection phase in normalized frequency of 0.315, and (c3) presents the −2nd reflection phase in normalized frequency of 0.552. The corresponding frequencies are marked in (a2)–(c2) with dashed lines. The PC structure (Fig. 1) with $r=0.5a$ and $r_s=0.4a$.

known that light cannot propagate in a PC when the frequency is inside the stop band. A wave vector k_z with a nonzero imaginary part is introduced to describe the stop band confinement, i.e., the field in the PC is evanescent along the z direction [24]. The situation is similar to dealing with total internal reflection between two homogeneous media. The perturbation-to-surface layer will make the field redistributed in the PC to meet Maxwell equations; as a result, it will affect the reflection phase for the electromagnetic boundary conditions of continuity. Owing to the strongest field near the surface, the phase is sensitive to perturbation. By modulating the surface layer, phase shifts can be adjusted and designed.

We should mention the fact that the symmetry of the reflection phase and the reflectance remain, even if the radii of the cylinders change. It would not be difficult to understand, since the displacement periodicity along the surface of the PC remains when the radii of the surface cylinders are changed.

4. GIANT GH SHIFT

As mentioned before, superluminal propagation and a giant GH shift from a PC can be achieved by modifying the phase. As an example, the giant GH shift is described here.

By designing the reflection phase, the giant GH shift is achieved for reflected light inside a stop band. For an incident beam that is sufficiently wide $\Delta k \ll k$, the GH shift of a reflected beam can be calculated analytically as $-d\phi(k_x)/dk_x$ [8–14]. Here, we consider the 2D PC (shown as Fig. 1) illuminated by a Gaussian beam with a finite width. The incident beam can be expressed by [10]

$$E^{(i)}(z,x) = \frac{1}{\sqrt{2\pi}} \int A(k_x)\exp[i(k_z z + k_x x)]\mathrm{d}k_x, \qquad (2)$$

where $A(k_x)=(W_x/\sqrt{2})\times\exp[-W_x^2(k_x-k_0\sin\theta_i)^2/4]$ is the angular spectrum of the Gaussian beam centered at $x=0$ on the plane of $z=0$, and W_x is the waist of the Gaussian beam. Then the reflected beam is given by

$$E^{(r)}(z,x) = \frac{1}{\sqrt{2\pi}} \int r^{(m)}(k_x)A(k_x)\exp[i(-k_z z + k_x x)]\mathrm{d}k_x. \qquad (3)$$

Since the center of the incident beam is at $x=0$, the GH shift (the displacement between the centers of the incident and reflected beams) can be calculated by

$$G = \int_{-\infty}^{+\infty} x|E^{(r)}(0,x)|^2\mathrm{d}x \Big/ \int_{-\infty}^{+\infty} |E^{(r)}(0,x)|^2\mathrm{d}x. \qquad (4)$$

Here, the PC structure is the same as that in Fig. 5, i.e., with a modified surface layer ($r=0.5a$, $r_s=0.4a$). The beam width W_x of the incident Gaussian beam is $25a$. The GH shift of the 0th order reflected light as a function of frequency and k_x is shown in Fig. 6. Inside the first stop band, maximum giant GH shifts of about $\pm 30a$ appear in some areas, while in other areas the GH shift is almost $0a$. The area with giant GH shifts in Fig. 6 corresponds to the concave in Fig. 5 with bigger $|-\mathrm{d}\phi(k_x)/\mathrm{d}k_x|$. It indicates that a well-designed reflection phase is constructive to achieve a giant GH shift. The inset shows the GH shift as a function of k_x in a normalized frequency of 0.315. The appearance of a giant GH shift for a 0th reflected wave can be explained by the existence of a high-order amplified evanescent wave. When the incident light is reflected by the surface of a PC, a high-order evanescent wave is stimulated and part of the energy is transferred from the incident light to an evanescent wave. Accompanying the propagating of evanescent waves along the surface for-

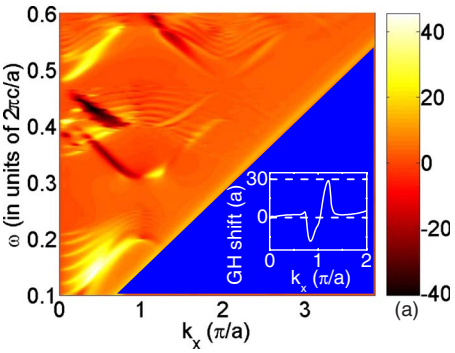

Fig. 6. (Color online) GH shift of the 0th order reflected wave as a function of frequency and k_x. The PC structure with $r=0.5a$, $r_s=0.4a$. The incident Gaussian beam width $W_x=25a$. The incident wave is an evanescent wave to be neglected. The inset shows the GH shift as a function of k_x in a normalized frequency of 0.315.

ward or backward, the energy is transferred back to a 0th order reflected wave gradually, and the center of the reflected beam shifts forward or backward correspondingly.

5. SUMMARY

In summary, we present an investigation on the reflection phase of a 2D PC. The phase shift of the $-m$th order reflected light is symmetric with respect to line $k_x = m\pi/b$ in the frequency-wave vector domain. The phase can be modulated by modifying the surface layer. Our investigation provides a robust way to design the reflection phase, from which giant positive or negative GH shifts are obtained.

ACKNOWLEDGMENTS

The authors acknowledge the financial support from the National Natural Science Foundation of China (NNSFC) grants 60908040 and 10974060 and the Natural Science Foundation of Guangdong Province of China grant 9451063101002256. This work is also supported by a grant from the Ph.D. Programs Foundation of Ministry of Education of China (No. 20094407120011).

REFERENCES

1. L. Brillouin, *Wave Propagation and Group Velocity* (Academic, 1960).
2. L. D. Landau and E. M. Lifshitz, *Electrodynamics of Continuous Media* (Pergamon, 1960).
3. M. Born and E. Wolf, *Principles of Optics*, 7th ed. (Cambridge U. Press, 1999).
4. G. Nimtz, A. Haibel, and R.-M. Vetter, "Pulse reflection by photonic barriers," Phys. Rev. E **66**, 037602 (2002).
5. D. R. Solli, C. F. McCormick, and R. Y. Chiao, "Fast light, slow light, and phase singularities: a connection to generalized weak values," Phys. Rev. Lett. **92**, 043601 (2004).
6. H. G. Winful, "Nature of 'superluminal' barrier tunneling," Phys. Rev. Lett. **90**, 023901 (2003).
7. L.-G. Wang, H. Chen, and S.-Y. Zhu, "Superluminal pulse reflection and transmission in a slab system doped with dispersive materials," Phys. Rev. E **70**, 066602 (2004).
8. I. Shadrivov, A. Zharov, and Y. S. Kivshar, "Giant Goos–Hänchen effect at the reflection from left-handed metamaterials," Appl. Phys. Lett. **83**, 2713–2715 (2003).
9. X. Yin, L. Hesselink, Z. Liu, N. Fang, and X. Zhang, "Large positive and negative lateral optical beam displacements due to surface plasmon resonance," Appl. Phys. Lett. **85**, 372–374 (2004).
10. L. G. Wang and S. Y. Zhu, "Giant lateral shift of a light beam at the defect mode in one-dimensional photonic crystals," Opt. Lett. **31**, 101–103 (2006).
11. H. M. Lai and S. W. Chan, "Large and negative Goos–Hänchen shift near the Brewster dip on reflection from weakly absorbing media," Opt. Lett. **27**, 680–682 (2002).
12. D. Felbacq and R. Smaâli, "Bloch modes dressed by evanescent waves and the generalized Goos–Hänchen effect in photonic crystals," Phys. Rev. Lett. **92**, 193902 (2004).
13. J. He, J. Yi, and S. He, "Giant negative Goos–Hänchen shifts for a photonic crystal with a negative effective index," Opt. Express **14**, 3024–3029 (2006).
14. R. Gruschinski, G. Nimtz, and A. A. Stahlhofen, "Resonance-like Goos–Hänchen shift induced by nanometal films," Ann. Phys. **17**, 917–921 (2008).
15. Z.-Y. Li and K.-M. Ho, "Light propagation in semi-infinite photonic crystals and related waveguide structures," Phys. Rev. B **68**, 155101 (2003).
16. E. Istrate, A. A. Green, and E. H. Sargent, "Behavior of light at photonic crystal interfaces," Phys. Rev. B **71**, 195122 (2005).
17. E. Istrate and E. H. Sargent, "Measurement of the phase shift upon reflection from photonic crystals," Appl. Phys. Lett. **86**, 151112 (2005).
18. M. Golosovsky, Y. Neve-Oz, and D. Davidov, "Phase shift on reflection from metallodielectric photonic bandgap materials," Phys. Rev. B **70**, 115105 (2004).
19. Q. F. Dai, Y. W. Li, and H. Z. Wang, "Broadband two-dimensional photonic crystal wave plate," Appl. Phys. Lett. **89**, 061121 (2006).
20. G. Freymann, W. Koch, D. C. Meisel, M. Wegener, M. Diem, A. Garcia-Martin, S. Pereira, K. Busch, J. Schilling, R. B. Wehrspohn, and U. Gösele, "Diffraction properties of two-dimensional photonic crystals," Appl. Phys. Lett. **83**, 614–616 (2003).
21. D. Maystre, "Photonic crystal diffraction gratings," Opt. Express **8**, 209–216 (2001).
22. D. Labiloy, D. Labilloy, H. Benisty, C. Weisbuch, T. F. Krauss, D. Cassagne, C. Jouanin, R. Houdré, U. Oesterle, and V. Bardinal, "Diffraction efficiency and guided light control by two-dimensional photonic-bandgap lattices," IEEE J. Quantum Electron. **35**, 1045–1052 (1999).
23. R. M. Bell, J. B. Pendry, L. Martin Moreno, and A. J. Ward, "A program for calculating photonic band structures and transmission coefficients of complex structures," Comput. Phys. Commun. **85**, 306–322 (1995).
24. M. Ibanescu, E. J. Reed, and J. D. Joannopoulos, "Enhanced photonic bandgap confinement via Van Hove saddle point singularities," Phys. Rev. Lett. **96**, 033904 (2006).